JOURNAL OF GEOPHYSICAL RESEARCH, VOL. 109, C01007, doi:10.1029/2003JC002014, 2004

An adjoint sensitivity study of chlorofluorocarbons in the North Atlantic

Xingwen Li[1]

MIT/WHOI Joint Program in Physical Oceanography, Massachusetts Institute of Technology, Cambridge, Massachusetts, USA

Carl Wunsch

Department of Earth, Atmospheric and Planetary Sciences, Massachusetts Institute of Technology, Cambridge, Massachusetts, USA

Received 23 June 2003; revised 28 August 2003; accepted 9 October 2003; published 3 January 2004.

[1] Adjoint sensitivities of CFC-11 concentrations and CFC-11/CFC-12 ratio ages in a North Atlantic general circulation model are analyzed. These sensitivities are compared with those of spiciness, $T - (\beta/\alpha)\, S$, where α, β are the thermal and haline expansion coefficients, respectively. High-sensitivity fields are candidates for providing the most powerful constraints in the corresponding inverse problems. In the dual (adjoint) solutions all three variables exhibit the major ventilation pathways and define the associated timescales in the model. Overall, however, spiciness shows the highest sensitivity to the flow field. In the North Atlantic Deep Water, sensitivities of CFC properties and spiciness to the isopycnal mixing and thickness diffusion are of the same order of magnitude. In the lower subtropical thermocline, sensitivities of CFC properties to the isopycnal mixing and thickness diffusion are higher. The utility of this sensitivity is undermined by the need to reconstruct their boundary conditions. Given the influence of T, S measurements on the density field, they produce the most powerful constraints on the model on the large scale. It still remains possible, however, that transient tracers can provide a larger relative information content concerning the mixing process between the near-surface boundary layer and the thermocline but dependent upon the ability to reconstruct accurate initial and boundary conditions. *INDEX TERMS:* 4294 Oceanography: General: Instruments and techniques; 4532 Oceanography: Physical: General circulation; 4271 Oceanography: General: Physical and chemical properties of seawater; 4255 Oceanography: General: Numerical modeling; *KEYWORDS:* transient tracers, state estimation, adjoint sensitivity

Citation: Li, X., and C. Wunsch (2004), An adjoint sensitivity study of chlorofluorocarbons in the North Atlantic, *J. Geophys. Res.*, *109*, C01007, doi:10.1029/2003JC002014.

1. Introduction

[2] Oceanic parameters such as mixing rates and flow fields have long been estimated from quasi-steady tracer data (e.g., temperature, salinity, and oxygen) and other conventional measurements [e.g., *Wunsch*, 1996, hereinafter referred to as W96; *Ganachaud and Wunsch*, 2003]. More recently, observations of transient tracers have become comparatively common and some attempts have been made to make inferences about the ocean using these temporally evolving fields [e.g., *Kelley and Van Scoy*, 1999; *Haine et al.*, 1998; *Smethie and Fine*, 2001; *Rhein et al.*, 2002] with a variety of methods and assumptions.

[3] The most general approach to using transient tracer data is to regard them simply as another generic data set, much like current meter or altimetric data, and to employ the inverse methods of time-dependent state estimation which have now become practical [*Stammer et al.*, 2002, 2003; *Fukumori et al.*, 1999; W96]. As a step toward that most general approach, *Li and Wunsch* [2003, hereinafter referred to as paper 1] constrained a so-called off-line North Atlantic Ocean model (an advection-diffusion model with the flow field computed from a full general circulation model (GCM)) with tritium and chlorofluorocarbon (CFC) data and showed that the model could be brought into consistency with the transient tracer fields. (The model was, however, inadequate in the convective high-latitude region of the ocean, and a reduced area was then employed.) Consistent, however, with earlier simpler studies [e.g., *Mémery and Wunsch*, 1990; *Gray and Haine*, 2001], most of the information content of the transient tracers was soaked up in adjusting the uncertain transient tracer boundary conditions, rather than constraining either oceanic flow or mixing coefficients. We refer to paper 1 for the details of these computations.

[1]Now at Applied Ocean Physics and Engineering Department, Woods Hole Oceanographic Institution, Woods Hole, Massachusetts, USA.

0148-0227/04/2003JC002014$09.00

[4] Given that there nonetheless appear to be no particular obstacles or difficulties in employing transient tracers in general oceanic state estimation procedures, we here address a more fundamental question: to what extent do transient tracers uniquely provide information about the large-scale ocean circulation? The question is of practical interest both for existing data not yet used, and for the development of future field programs. For example, oceanic state estimation is labor intensive involving, among other issues, the production of reasonably accurate estimates of data and model errors. To the extent that transient tracer data are likely to provide important constraints in addition to more conventional ones, undertaking their use becomes very important. We distinguish this question from that pertaining to the physics of the very upper ocean, an issue we return to at the end.

[5] Our focus here is on the nonequatorial North Atlantic Ocean. Transient tracers have also been used to infer equatorial flows and interhemispheric exchange [e.g., *Weiss et al.*, 1985; *Rhein et al.*, 1998; *Andrie et al.*, 1998; *Messias et al.*, 1999]. It is possible, as with the surface layers, that in regions of strong ageostrophic flows, transient tracers will prove uniquely valuable, but such an inference can only be made from models with adequate resolution. Low latitudes are beyond our current scope.

[6] The sensitivity of various, representative, elements of the ocean circulation to the distributions and concentrations of realistic transient tracers are studied here. A method based upon the ability to determine the partial derivatives of various objective (or cost) functions to data perturbations is used. These partial derivatives are available to us through the adjoint of the off-line general circulation model. That model adjoints provide sensitivity information has been long known in the general optimization literature, and has been exploited in the atmospheric and oceanic contexts [e.g., *Hall and Cacuci*, 1983; *Galanti et al.*, 2002; *Huang et al.*, 2003; W96, pp. 362–372]. *Marotzke et al.* [1999] described the specific approach that we use here, one in turn based upon the automatic differentiation tool of *Giering and Kaminski* [1998].

[7] CFC-11 and CFC-12 are perhaps the simplest transient tracers to be incorporated in a model, as their source functions are comparatively well known. *Robbins et al.* [2000] argued that a single tracer property was not sensitive to discerning the effects of diffusive versus advective ventilation; the use of coupled transient tracers, such as tracer age, might provide greater sensitivity to diffusive effects. Thus the sensitivities of both CFC-11 concentration and τ, the CFC-11/CFC-12 ratio age, are computed.

[8] Sensitivities can only be interpreted relative to those of other data types. As a comparison standard, we use conventional steady tracer distributions, in particular temperature, T, and salinity, S, which are the most widely available and best understood of all oceanic tracers. Other possibilities exist, including nutrient, and oxygen tracers, but any approach to their rigorous use involves modeling the biogeochemical processes in which they are involved. T, S are dynamically active, directly affecting the density and hence the flow field. To use them therefore in a more straightforward comparison with the passive transient tracers, we will form "spiciness",

$$\pi = \alpha T - \beta S.$$

[*Veronis*, 1972; *Munk*, 1981]. To a linear approximation of the equation of state, π has no affect on density. In practice, it is here slightly more convenient to use,

$$\pi' = T - (\beta/\alpha)S. \tag{1}$$

2. Model Description

[9] The forward model and its adjoint are identical to those in paper 1, with the exception that the meridional domain is extended from 4.5°S–78.5°N. As will be seen, including the high-latitude region, which was excluded in paper 1, does not affect the interior sensitivity results. This model solves an advection-diffusion equation of form,

$$\frac{\partial C}{\partial t} + \mathbf{u}\cdot\nabla C - \nabla\cdot(\mathbf{K}\nabla C) = -\lambda C + q, \tag{2}$$

where q represents sinks/sources, λ is a decay constant, $\mathbf{u}$ is velocity, $\mathbf{K}$ is a mixing tensor, and together defining the off-line model. In this off-line model, CFC properties and π' are all treated as passive tracers. The mixing parameters, the three-dimensional velocities and the initial tracer fields are thereby control variables that govern the tracer distributions.

[10] Horizontal resolution of the model is $1^\circ \times 1^\circ$ with 21 vertical levels ranging from 25 m at the surface to 500 m near the ocean bottom. Realistic topography is employed. Parts of the northern, eastern, and southern boundaries are open, where nonzero tracer fluxes are permitted. Paper 1 should be consulted for additional details.

3. Boundary Conditions

[11] For specificity, we use CFCs as representative of transient tracers with decadal timescales. A different analysis with much longer runs would be required for direct study of tracers with thousand-year plus adjustment times (but even CFCs require many decades to reach equilibrium [see *Wunsch*, 2002]). CFC fluxes across the ocean surface are computed as,

$$F = K_w(C_e - C_s), \tag{3}$$

where C_s is the modeled sea surface tracer concentration, C_e the oceanic surface equilibrium value, and K_w is an empirical coefficient. Uncertainties in the CFC fluxes are mainly due to the uncertainties in K_w, and its multiplicative nature largely absorbs the remaining errors in C_e, C_s. A monthly climatology of K_w is computed from the equation,

$$K_w = (1 - F_i)\left[a\left(u_w^2 + \sigma_w^2\right)\right](Sc/660)^{-1/2}, \tag{4}$$

[*Wanninkhof*, 1992]. Here F_i is the fraction of the local sea surface covered with ice; u_w is the monthly climatological surface wind speed; σ_w^2 is the variance of u_w; a is a constant; Sc is the Schmidt number. More details can be found at http://www.ipsl.jussieu.fr/OCMIP.

[12] Lateral boundary concentrations of CFCs are from a global run of the MIT GCM [*Dutay et al.*, 2002]. The initial conditions are CFC concentrations on 1 January 1950 in a forward model run, which starts from a zero CFC back-

ground in 1940. τ is computed from the modeled CFC-11 and CFC-12 concentrations, using the method by *Doney and Bullister* [1992].

[13] Before 1950, CFC concentrations in the ocean were very small, and after 1980, the atmospheric CFC-11/CFC-12 ratio was no longer a monotonically increasing function of time [e.g., *Smethie et al.*, 2000, Figure 1]. This sensitivity study is thus confined to the time period 1950–1980.

[14] For π', the initial condition is its climatological state in January, obtained from the monthly climatological *T*, *S* fields in the online GCM. At the ocean surface and lateral boundaries, π' is restored toward the same monthly climatology.

4. Linearization and Interpretation

[15] The use of adjoint equations to determine sensitivity is now well known, and we summarize only briefly, following W96, *Marotzke et al.* [1999] and *Vautard et al.* [2000], using the notation of W96. The forward model (equation (2)) can be represented in a discrete form

$$\mathbf{x}_{n+1} = \mathbf{A}(\mathbf{x}_n, \mathbf{u}). \tag{5}$$

Here $\mathbf{x}_n$ is the state vector, (tracer concentration); $\mathbf{u}$ is the control vector, comprising the parameters that govern the tracer concentration; n is the time step, with $\Delta t = 1$. Consider a scalar objective function,

$$J = \frac{1}{N}\mathbf{b}^T\mathbf{x}_{t_f}, \tag{6}$$

where $\mathbf{x}_{t_f}$ is the state vector at the end time, and N is its dimension. Vector $\mathbf{b}$ is used to select subsets of the elements of $\mathbf{x}_{t_f}$ at particular locations (where the elements are one, otherwise they are zero).

[16] Then,

$$\delta J = \frac{1}{N}\mathbf{b}^T\delta\mathbf{x}_{t_f}. \tag{7}$$

The perturbation of $\mathbf{x}$ at any time step n can be obtained from equation (5),

$$\begin{aligned}\delta\mathbf{x}_{n+1} &= \left[\frac{\partial\mathbf{A}(\mathbf{x}_n,\mathbf{u})}{\partial\mathbf{x}_n}\Big|_{\mathbf{x}_n=\bar{\mathbf{x}}_n}\delta\mathbf{x}_n\right] + \left[\frac{\partial\mathbf{A}(\mathbf{x}_n,\mathbf{u})}{\partial\mathbf{u}}\Big|_{\mathbf{u}=\bar{\mathbf{u}}}\delta\mathbf{u}\right] \\ &= \mathbf{M}_n\delta\mathbf{x}_n + \mathbf{G}_n\delta\mathbf{u},\end{aligned} \tag{8}$$

where $\delta\mathbf{x}_n = \mathbf{x}_n - \bar{\mathbf{x}}_n$, with overbar representing the basic state, specifically here the four-dimensional tracer state in the model; $\mathbf{M}_n = \partial\mathbf{A}/\partial\mathbf{x}_n$; $\mathbf{G}_n = \partial\mathbf{A}/\partial\mathbf{u}$ at time step n. Equation (8) is a Taylor series expansion about a nominal solution, and is a linear model whose coefficients are determined by slopes tangent to the trajectories of the state variables and control variables in the forward model. It is a "tangent linear model".

[17] The final perturbation $\delta\mathbf{x}_{t_f}$ in equation (7) can be obtained from equation (8),

$$\begin{aligned}\delta\mathbf{x}_{t_f} &= \mathbf{M}_{t_f-1}\delta\mathbf{x}_{t_f-1} + \mathbf{G}_{t_f-1}\delta\mathbf{u} \\ &= \mathbf{M}_{t_f-1}\mathbf{M}_{t_f-2}..\mathbf{M}_0\delta\mathbf{x}_0 + \left(\mathbf{M}_{t_f-1}\mathbf{M}_{t_f-2}..\mathbf{M}_1\mathbf{G}_0\right. \\ &\quad \left. + \mathbf{M}_{t_f-1}\mathbf{M}_{t_f-2}..\mathbf{M}_2\mathbf{G}_1 + .. + \mathbf{M}_{t_f-1}\mathbf{G}_{t_f-2} + \mathbf{G}_{t_f-1}\right)\delta\mathbf{u}.\end{aligned} \tag{9}$$

If the control variables include the initial condition $\mathbf{x}_0$, and $\delta\mathbf{x}_0$ is incorporated in $\delta\mathbf{u}$, or $\delta\mathbf{x}_0 = 0$ (fixed initial condition),

$$\delta\mathbf{x}_1 = \mathbf{G}_0\delta\mathbf{u}. \tag{10}$$

In this special case, one can write an explicit relationship between the controls and $\delta\mathbf{x}_{t_f}$,

$$\delta\mathbf{x}_{t_f} = \mathbf{B}\delta\mathbf{u}. \tag{11}$$

Matrix $\mathbf{B}$ involves the sums of successive of $\mathbf{M}_n$ and $\mathbf{G}_n$ in equation (9).

[18] Substituting equation (11) into equation (7),

$$\delta J = \frac{1}{N}\mathbf{b}^T\mathbf{B}\delta\mathbf{u}, \tag{12}$$

or

$$\delta J = \left\langle\frac{\mathbf{B}^T\mathbf{b}}{N}, \delta\mathbf{u}\right\rangle, \tag{13}$$

where superscript T is the transpose, and $\langle\cdot\rangle$ is a scalar product.

[19] The sensitivity is defined as $\mathbf{B}^T\mathbf{b}/N$ and can be found numerically by integrating the adjoint model backward in time:

$$\left(\delta\mathbf{x}_{t_f}\right)^T = \left(\frac{\partial J}{\partial\mathbf{x}_{t_f}}\right)^T \tag{14}$$

$$\left(\delta\mathbf{u}_{t_f}\right)^T = 0 \tag{15}$$

$$\left(\delta\mathbf{x}_{n-1}\right)^T = \left(\delta\mathbf{x}_n\right)^T\left(\frac{\partial\mathbf{A}(\mathbf{x}_{n-1},\mathbf{u})}{\partial\mathbf{x}_{n-1}}\right)^T \tag{16}$$

$$\left(\delta\mathbf{u}_{n-1}\right)^T = \left(\delta\mathbf{u}_n\right)^T + \left(\delta\mathbf{x}_n\right)^T\left(\frac{\partial\mathbf{A}(\mathbf{x}_{n-1},\mathbf{u})}{\partial\mathbf{u}}\right)^T. \tag{17}$$

Therefore the sensitivity information propagates in the time-reversed direction by integration of the adjoint equations. The output $(\delta\mathbf{u}_0)^T$ is the sensitivity of the cost function to the control vector u at time $t = 0$. In this paper, backward integration refers to the period 1980–1950.

[20] (Conventional derivations are carried out for objective functions, *J*, that are quadratic in problem parameters. Although equation (6) is linear in the state vector, $\mathbf{x}_{t_f}$, the change can be shown to be immaterial here.)

5. Sensitivities of Tracer Properties in the NADW

[21] In this section, the sensitivities of the modeled tracer fields in the North Atlantic Deep Water (NADW) are analyzed. Figure 1 shows the modeled tracer distributions at 2200 m, approximately the central depth of the calculated NADW. The CFC-enriched, young and fresh NADW has clear imprints along the Deep Western Boundary. Both CFC properties and π' are carried along the

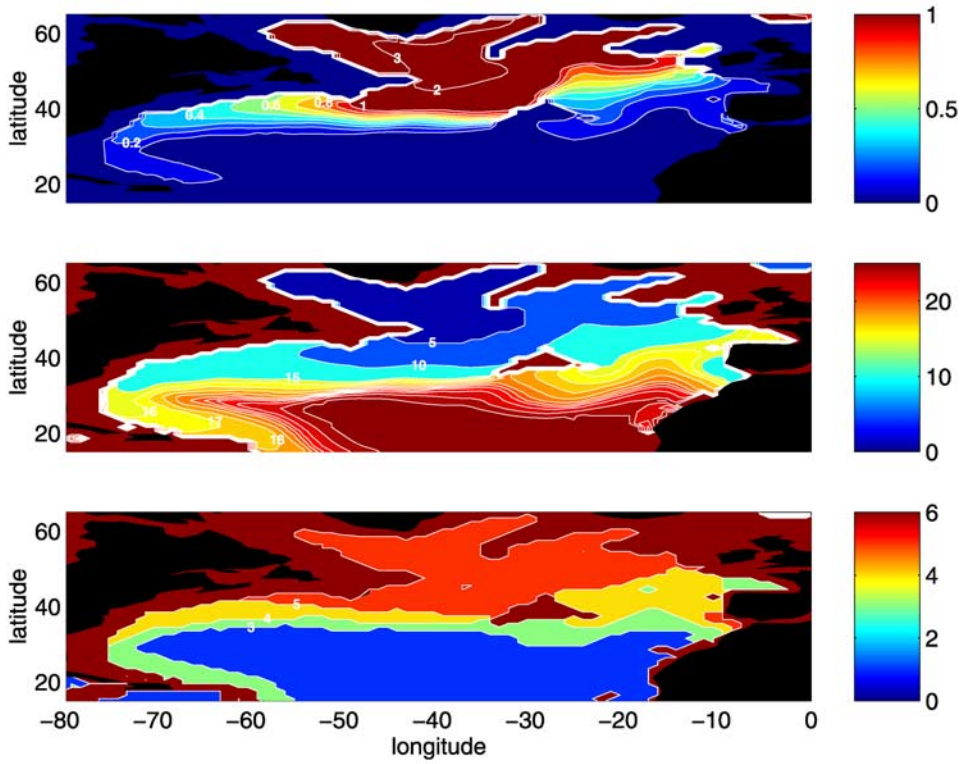

Figure 1. Distributions of the (top) modeled CFC-11 concentration (pmol/kg), (middle) τ (years), and (bottom) $\pi' + 120$ (°C) at 2200 m, June 1980. The scales of the color bars are chosen to let the southward spreading tongue near 30.5°N stand out. The overly active high-latitude convection carries too much surface property to depth too fast, as discussed in paper 1.

trajectory of the NADW, distributed by the same physical processes.

[22] The objective function here is,

$$J = \frac{1}{N}\sum_{i=1}^{N} C_i, \tag{18}$$

that is, the concentrations at the terminal time in June 1980 at 30.5°N, within the depth range 1335–2700 m and longitudes 80.5°–60.5°W. These samples are summed horizontally and vertically at each time step in June 1980. The summation is then divided by N, the number of total samples of each tracer property. J represents the approximate mean tracer property in the NADW at 30.5°N in June 1980.

[23] Sensitivities of different tracers are normalized for comparison by,

$$s = \frac{1}{\delta J_o}\frac{\partial J}{\partial \mathbf{u}}. \tag{19}$$

Here $\partial J/\partial \mathbf{u}$ is the adjoint model result, with the control variable, $\mathbf{u}$; it includes boundary conditions, flow fields and mixing coefficients; $\delta J_o = O(J)$. In Figure 1, the perturbations of tracer properties in the NADW at 30.5°N in June 1980 are $|\delta J_o|$ = 0.1 pmol/kg for CFC-11 concentration, $|\delta J_o|$ = 10 years for the CFC-11/CFC-12 ratio age, and $|\delta J_o|$ = 1°C for π'. For CFC-11 concentration or π', δJ_o is positive. As low values of CFC age (young water) are carried by the NADW, $\delta J_o = -10$ years for τ.

[24] The sensitivity to a model parameter can be interpreted as either the response of the objective function to a unit perturbation of the parameter or, conversely, the extent to which a value of the objective function (e.g., a model-data misfit) can constrain the parameter. The larger the sensitivity, the more rigidly the parameter can be constrained.

[25] Starting at the location where the cost function is evaluated, "information" propagates backward in time according to the physics of the adjoint model. The adjoint model solution demonstrates the pathways and times from which the terminal state arose. This information flow is perhaps most easily understood from a Green function point of view: in a conventional Green function representation, a disturbance at time t_0, at position $\mathbf{r}_0$, gives rise to a signal $G(t, \mathbf{r}|t_0, \mathbf{r}_0)$, $t \geq t_0$. One can determine the origins of an arbitrary disturbance at t, $\mathbf{r}$, by computing G for all possible t_0, $\mathbf{r}_0$; the number of model runs equals the number of locations $\mathbf{r}_0$ from which a disturbance can emanate and influence the result at $\mathbf{r}$. Alternatively, by the so-called reciprocity theorem, the function $G(t_0, \mathbf{r}_0|t, \mathbf{r})$, $t \geq t_0$ produces those locations t_0, $\mathbf{r}_0$ giving rise to a disturbance at t, $\mathbf{r}$. $G(t_0, \mathbf{r}_0|t, \mathbf{r}) = \tilde{G}(t, \mathbf{r}|t_0, \mathbf{r}_0)$ is the solution to the adjoint model [see, e.g., *Morse and Feshbach*, 1953, p.858]. Only a single backward computation of the adjoint model is required, defining the great power of this approach.

[26] Figure 2 shows the normalized sensitivities of the CFC-11 concentration to the meridional flow at 2200 m. Negative values in the north mean that the stronger the southward (negative) flow, the more CFC-11 enriched water

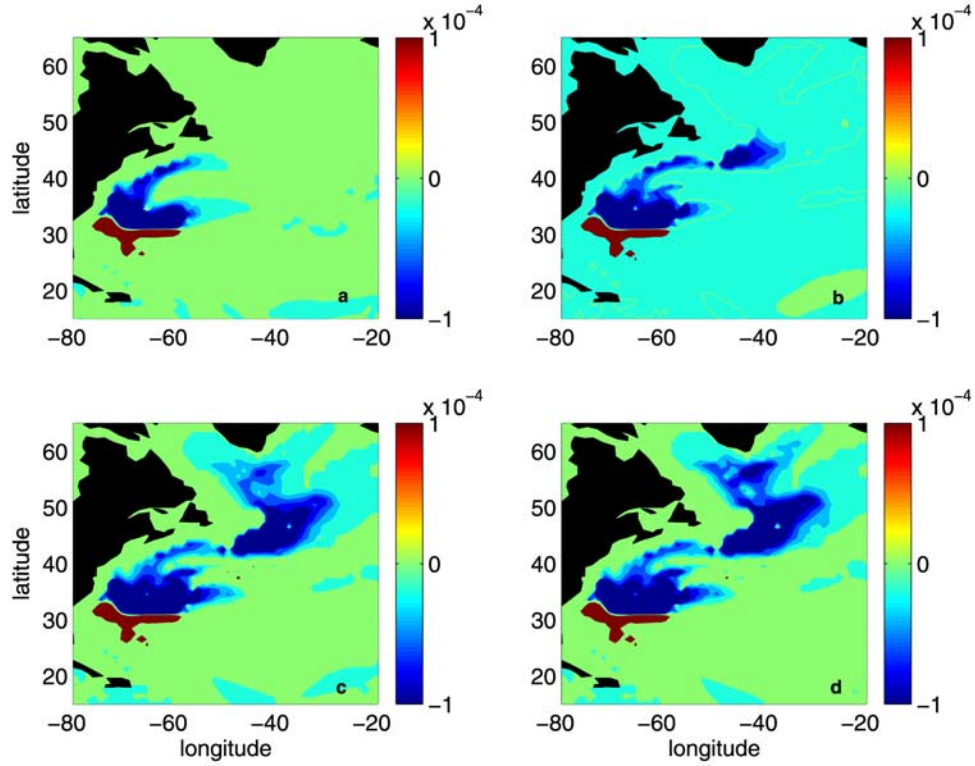

Figure 2. Normalized sensitivities of the CFC-11 concentration in the NADW between depths 1335 and 2700 m and longitudes 80.5° and 60.5°W at 30.5°N, June 1980, to the February meridional flow at 2200 m depth in (a) 1977, (b) 1973, (c) 1965, and (d) 1950. Units are $(\mathrm{cm/s})^{-1}$.

will be carried to 30.5°N from the high latitudes; positive values in the south mean that the stronger the southward flow, the more CFC-11 enriched water will be carried southward away from 30.5°N. Starting at 30.5°N, information propagates mainly upstream, northward along the western boundary. It takes about 6 years for a significant sensitivity signal to appear at the Grand Banks, corresponding to a mean transport speed of about 2 cm/s (*Wunsch* [2002] has pointed out that the ventilation time/speed is a very vague idea, depending on a threshhold value of the signal. Signals can propagate away quickly by fast waves in the system. *Marotzke et al.* [1999] see a communication between midlatitudes and the Labrador Sea within a year.) After 15 years (from 1980 to 1965) of integration, information reaches the Labrador Sea, where the modeled NADW originates. As the time of adjoint integration increases, the sensitivity in the Labrador Sea grows stronger. (However, the overactive convection there does not affect these downstream sensitivities.)

[27] Normalized sensitivities of τ and π', in Figure 3, exhibit similar advective pathways. Information is carried primarily northward along the western boundary with the same negative sign. Both transient and steady tracer properties at 30.5°N in the NADW take about 6 years to reach the Grand Banks, and 15 years to reach the Labrador Sea in the model [*Li*, 2003]. The negative values of the normalized sensitivity of the CFC age, presented in the opposite sign of $\partial J/\partial u$ (equation (19)), can be explained by the advective effect. A decrease of the southward flow in the region north of 30.5°N (carrying young water), or an increase of the northward flow in the region south of 30.5°N (carrying old water), leads to an increase of the cost function.

[28] Steady tracer π' provides the greatest sensitivity to the flow field, suggesting that observations of its distribution provide the strongest constraints upon the system. This result is an underestimate of the sensitivity: because the underlying (off-line) GCM is only marginally consistent with the T–S distribution, its sensitivity to π' constraints (related to geostrophic balance and used implicitly in the *Stammer et al.* [2002] calculations) should also be accounted for. Unlike T and S, CFCs do not appear in the GCM state vector and so do not carry this additional information about the flow field.

[29] In the forward direction, after being brought down by the deep convection, the tracer properties spread southward approximately along isopycnals. In the model, the isopycnal mixing and thickness diffusion are represented by the same parameter. The normalized sensitivities to the isopycnal and thickness diffusion at 2200 m are presented in Figure 4. High sensitivities are concentrated upstream. Each tracer exhibits a similar pathway: a band of large values along the western boundary. The amplitudes of the normalized sensitivities have the same order. No obvious advantage relative to π' is seen in the use of the CFC properties in constraining the mixing rates in the NADW.

6. Lower Subtropical Thermocline Ventilation

[30] Several studies, using tracer data, exist of the mechanisms contributing to the ventilation of the lower subtrop-

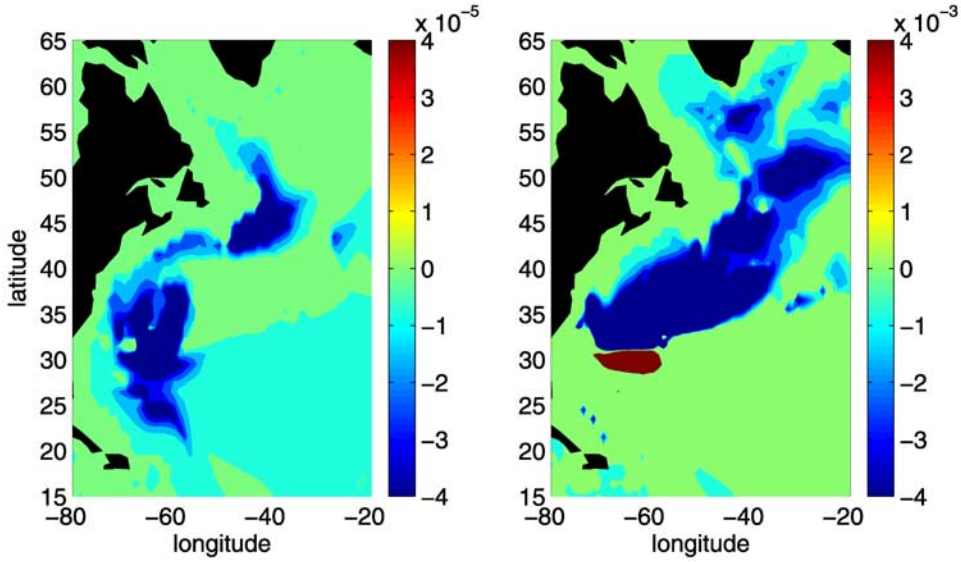

Figure 3. Normalized sensitivities of (left) τ and (right) π' in the NADW between depths 1335 and 2700 m and longitudes 80.5° and 60.5°W at 30.5°N, June 1980, to the February meridional flow at 2200 m depth in 1950. Scales of the color bars are different. The sensitivity of π' is much stronger everywhere. Units are $(\text{cm/s})^{-1}$.

ical thermocline in the North Atlantic, [e.g., *Robbins et al.*, 2000; *Roether and Fuchs*, 1988]. We again, however, seek to compare sensitivities of the ventilation values to hydrographic and transient tracer data.

[31] The objective function is in the same form in equation (18), except that it now represents modeled tracer samples between 510 and 710 m depths and 60.5° and 20.5°W longitudes at 30.5°N, in June 1980. Because vertical layer thickness at 510 m in the model is 75% of the layer thickness at 710 m, the mean tracer properties are slightly weighted toward values at 510 m.

[32] Modeled tracer distributions at 510 m are shown in Figure 5. The distribution patterns of CFC properties are similar: surface values invade the subtropical area from its northeast corner and penetrate southwestward across the gyre. The distribution of π' is different. Its isolines are more consistent with streamlines. Recirculation of the subtropical gyre is evident in the closed isolines of high values, and the western boundary current and its extension are apparent through the compression of isolines.

[33] Three basic mechanisms exist that can ventilate the subtropical thermocline: directly, due to Ekman pumping; passage of recirculating waters through areas of deep winter convection; and diffusive ventilation from isopycnal mixing near the outcrops. In the model, the isopycnals outcrop at the surface at latitudes 43°–55°N in the eastern basin. The Azores Current, which blocks the direct advective ventilation of lower subtropical thermocline by *Robbins et al.* [2000], is absent in the $1° \times 1°$ model.

[34] Normalization factors, δJ_o in equation (19), are taken to be 1 pmol/kg for CFC-11 concentration, −1 year for τ, and −10°C for π' (see Figure 5). δJ_o is negative for the CFC age and π', because low values are carried by the ventilated water from the northeast corner of the subtropical gyre.

[35] The sensitivities are forced by the monthly mean tracer perturbations in June 1980, between depths 510–

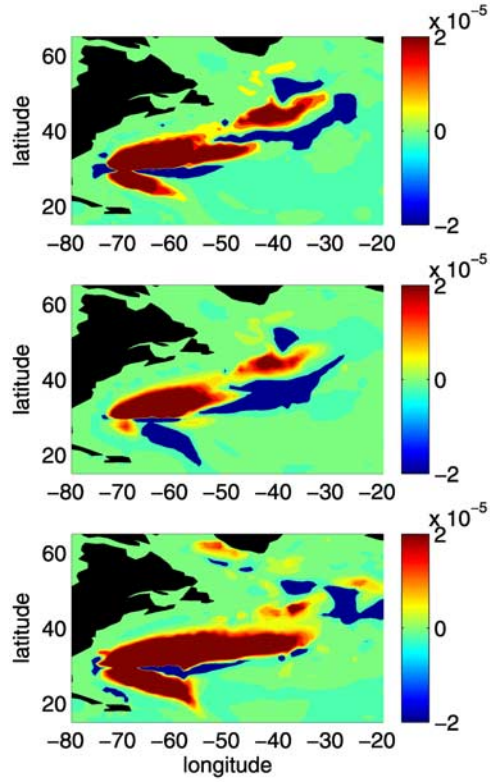

Figure 4. Normalized sensitivities of the (top) CFC-11 concentration, (middle) τ, and (bottom) π' in the NADW between depths 1335 and 2700 m and longitudes 80.5° and 60.5°W at 30.5°N, June 1980, to the isopycnal mixing and thickness diffusion at 2200 m depth in 1950. Units are $(100\ \text{m}^2/\text{s})^{-1}$.

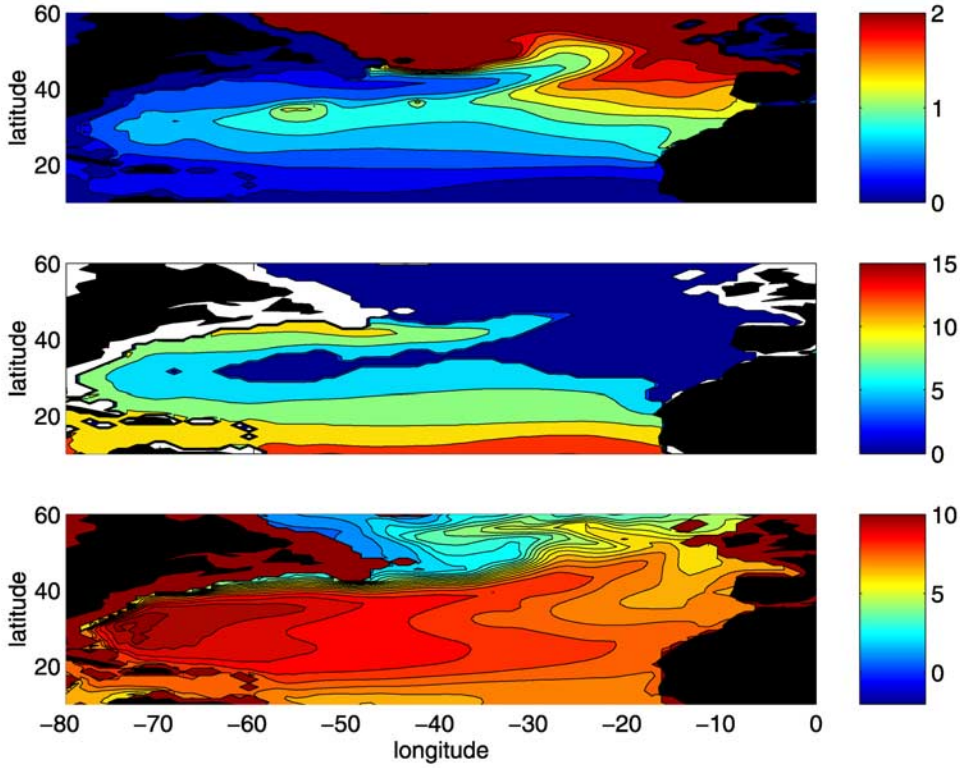

Figure 5. Distributions of the (top) modeled CFC-11 concentration (pmol/kg), (middle) τ (year), and (bottom) $\pi' + 120$ (°C) at 510 m depth, June 1980.

710 m at 30.5°N. Information then propagates upstream in the backward integration of the adjoint model. Figure 6 shows the normalized sensitivities of the tracer properties to the meridional velocity at 40.5°W in 1950. Information spreading approximately along isopycnals is visible. Sensitivity of π' to meridional velocity perturbations is again the largest. Advective sensitivity of CFC-11 concentration in the lower thermocline is the weakest.

[36] Figure 7 shows the normalized sensitivities of the tracer properties to the isopycnal mixing and thickness diffusion at 40.5°W after 30 years of backward information flow. Positive values spread northward approximately along isopycnals, demonstrating the ventilation pathway. There are weak minima just south of 30.5°N. North of the section, mixing conveys the CFC-enriched young water, while south of 30.5°N, mixing transmits the CFC-deficient older water. During the 30 years integration, no appreciable sensitivity has appeared in the outcrop region. Sensitivities to the surface values are thus weak. Propagation pathways of different tracer properties are basically similar but not identical, because their boundary conditions and interior distributions in the ocean are different. Identification of second-order differences in the propagation speeds depends on chosen threshold values. In the presence of diffusion, this identification would be a poor idea [*Wunsch*, 2002].

[37] In contrast with the results for NADW, here the normalized sensitivity of τ is stronger than that of the CFC-11 concentration, consistent with the result of *Robbins et al.* [2000]. π' in turn shows a weaker sensitivity to the isopycnal and thickness diffusion than does the CFC properties, in the lower subtropical thermocline.

[38] τ exhibits a greater sensitivity to diffusion parameterizations than does π', an important result. One might conclude therefore that τ should be used to determine mixing rates in models. In principle, this conclusion is correct. In practice unfortunately, assimilation of transient tracer observations in the North Atlantic between 4.5°S–39.5°N shows that most information in the data is absorbed in their uncertain boundary conditions (Paper 1). Sensitivity cannot be interpreted independent of the accuracy with which the fields are determined from observations. In particular, for quasi-steady tracers such as *T*, *S*, any uncertainty in a boundary condition can be reduced by obtaining further surface data at any time, including variations with the mean seasonal cycle. One cannot so reconstruct a poorly known transient tracer boundary condition from an earlier time. It remain possible, however, that transient tracers may provide a larger relative information content concerning the mixing process between the near-surface boundary layer and the thermocline, as well as the much less clearly observed near-surface boundary itself. Such a study is beyond our present scope as it requires extremely fine near-surface resolution and higher-order dynamics, an issue also mentioned in paper 1.

7. Summary and Discussion

[39] The adjoint sensitivities of CFC-11 concentration and CFC-11/CFC-12 ratio age in the North Atlantic are analyzed and compared with those of the steady tracer, π'. Sensitivities of the tracer properties in the NADW propagate mainly along the deep western boundary, consistent with the

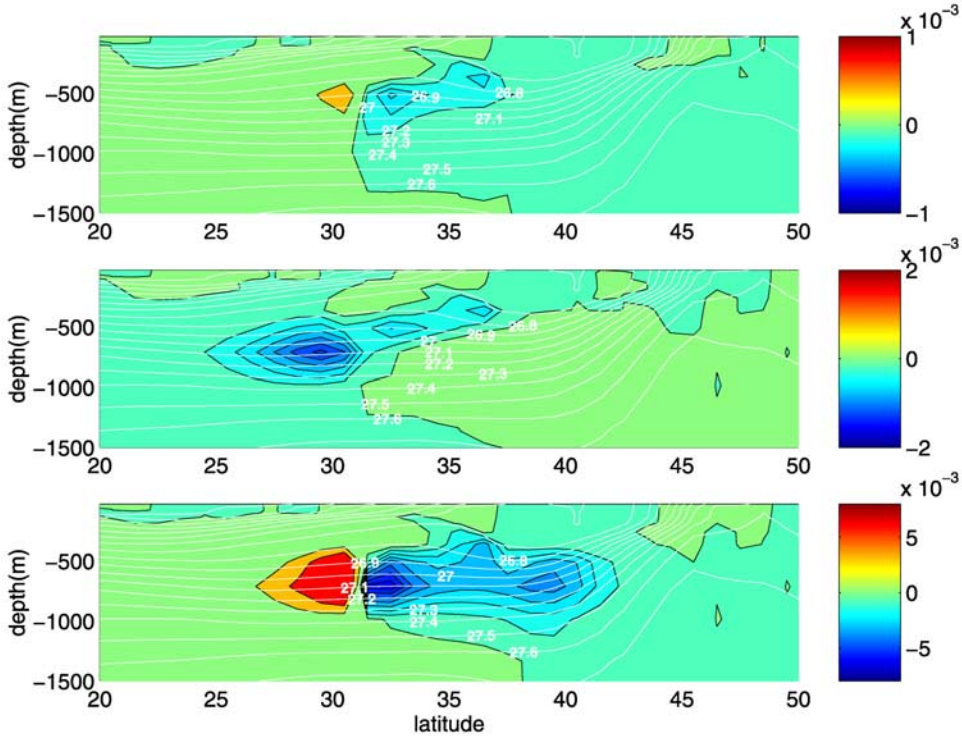

Figure 6. Normalized sensitivity of the (top) CFC-11 concentration, (middle) τ, and (bottom) π' in the lower subtropical thermocline between depths 510 and 710 m and longitudes 60.5° and 20.5°W at 30.5°N in 1980 to the February meridional flow at 40.5°W in 1950. Units are $(\text{cm/s})^{-1}$. White lines represent the potential density and hereafter in this section.

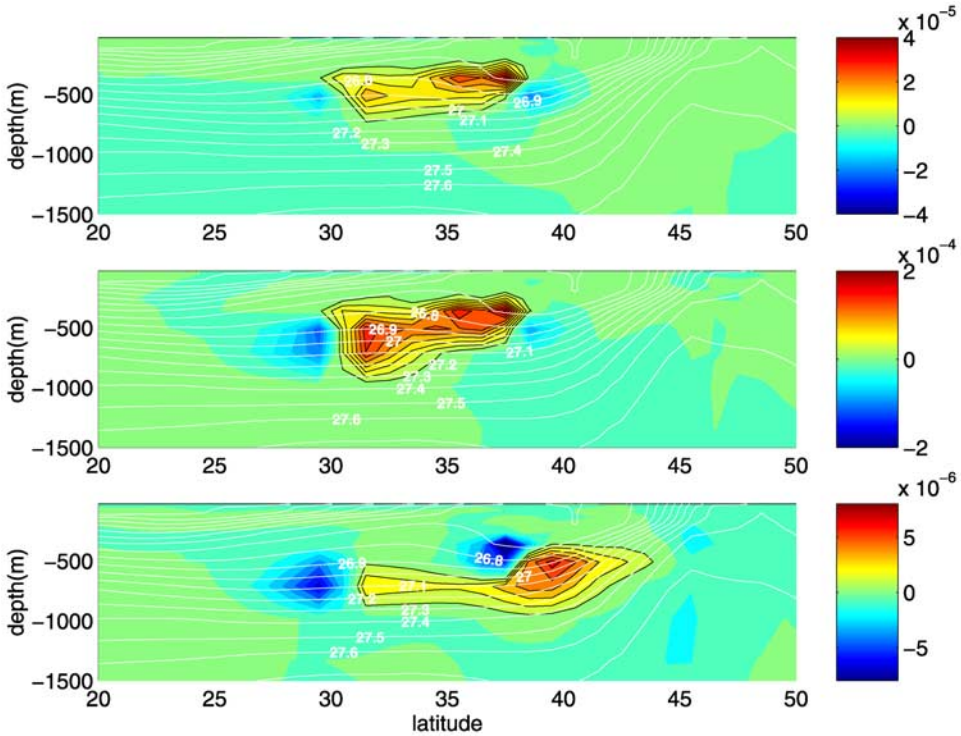

Figure 7. Normalized sensitivity of the (top) CFC-11 concentration, (middle) τ, and (bottom) π' in the lower subtropical thermocline between depths 510 and 710 m and longitudes 60.5° and 20.5°W at 30.5°N in 1980 to the isopycnal mixing and thickness diffusion at 40.5°W in 1950. Units are $(100\ \text{m}^2/\text{s})^{-1}$.

ventilation pathway of the NADW. In the adjoint model, it takes about 15 years for either transient or steady tracer signal in the NADW at 30.5°N to reach the Labrador Sea. In the lower subtropical thermocline, sensitivities show a similar ventilation pathway along isopycnal surfaces. Over 30 years of integration, substantial signals from neither transient and steady tracers have arrived at the surface winter outcrop region, from 30.5°N in the lower thermocline.

[40] In spite of different surface boundary conditions and oceanic distributions, the sensitivities of both steady and transient tracer properties successfully exhibit the ventilation pathways and the associated timescales in the model, and thereby can provide information to constrain the corresponding model physics. In a real state estimation procedure, both steady and transient tracers, once having entered a model, propagate under (nearly) the same dynamic rules. The corresponding sensitivity, such as that for a model-data misfit, then provides information about problematic transport pathways and timescales mainly upstream, and serves as a guide for the adjoint model to optimize its parameters. (T, S perturbations, if sufficiently large, will influence the flow field, a sensitivity not found in the CFCs and their equivalents.)

[41] Quantitatively, the steady spiciness tracer π' exhibits the strongest sensitivity to the flow field among all the tracer properties at all depths studied. Coupled with the generally accurately determined boundary conditions on T, S which define π', the implication is that hydrographic data are the better determinant of the advective fields relative to CFC-based data. In the lower thermocline, diffusion/mixing parameters appear to be more sensitive to τ, the CFC ratio age, but the practical use of these data is greatly complicated by unrecoverable uncertainties in the surface boundary conditions of the CFCs. It still remains possible that transient tracers may provide a larger relative information content concerning the mixing process between the near-surface boundary layer and the thermocline, but dependent upon the ability to reconstruct accurate initial and boundary conditions. More generally, invoking the conclusions of paper 1, there is no obstacle to using transient tracer data in constraining general circulation models. The actual uncertainties of transient tracer data, coupled with the generally lower sensitivity of the model state to these data, implies that the impact on the estimated state uncertainty will be less than might have been anticipated.

[42] **Acknowledgments.** This work was supported by NSF Award OCE-9730071, OCE-9617570, NASA Award NAG5-7857 and NAG5-11933. S. Doney provided the scripts for computing the CFC age. M. Follows explained the essential details of the construction of the adjoint model. The comments of two anonymous reviewers were helpful. This research has made use of the high performance computational system (Cray Sv1) at the Texas Advanced Computing Center through the National Partnership for Advanced Computational Infrastructure (NPACI).

References

Andrie, C., J.-F. Ternon, M.-J. Messias, L. Memery, and B. Bourles (1998), Chlorofluoromethane distributions in the deep equatorial Atlantic during January–March 1993, *Deep Sea Res., Part I*, *45*, 903–930.

Doney, S. C., and J. L. Bullister (1992), A chlorofluorocarbon section in the eastern North Atlantic, *Deep Sea Res., Part I*, *39*, 1857–1883.

Dutay, J. C., et al. (2002), Evaluation of ocean model ventilation with CFC-11: Comparison of 13 global ocean models, *Ocean Modell.*, *4*, 89–120.

Fukumori, I., R. Raghunath, L.-L. Fu, and Y. Chao (1999), Assimilation of TOPEX/Poseidon altimeter data into a global ocean circulation model: How good are the results?, *J. Geophys. Res.*, *104*, 25,647–25,665.

Galanti, E., E. Tziperman, M. Harrison, A. Rosati, R. Giering, and Z. Sirkes (2002), The equatorial thermocline outcropping—A seasonal control on the tropical Pacific ocean-atmosphere instability strength, *J. Clim.*, *15*, 2721–2739.

Ganachaud, A., and C. Wunsch (2003), Large-scale ocean heat and freshwater transports during the World Ocean Circulation Experiment, *J. Clim.*, *16*, 696–705.

Giering, R., and T. Kaminski (1998), Recipes for adjoint code construction, *Trans. Math. Software*, *24*, 437–474.

Gray, S. L., and T. W. N. Haine (2001), Constraining a North Atlantic ocean general circulation model with chlorofluorocarbon observations, *J. Phys. Oceanogr.*, *31*, 1157–1181.

Haine, T. W. N., A. J. Watson, M. I. Liddicoat, and R. R. Dickson (1998), The flow of Antarctic Bottom Water to the southwest Indian Ocean estimated using CFCs, *J. Geophys. Res.*, *103*, 27,637–27,653.

Hall, M. C. B., and D. G. Cacuci (1983), Physical interpretation of the adjoint functions for sensitivity analysis of atmospheric models, *J. Atmos. Sci.*, *40*, 2537–2546.

Huang, B., P. H. Stone, and C. Hill (2003), Sensitivities of deep-ocean heat uptake and heat content to surface fluxes and subgrid-scale parameters in an ocean general circulation model with idealized geometry, *J. Geophys. Res.*, *108*(C1), 3015, doi:10.1029/2001JC001218.

Kelley, D. E., and K. A. Van Scoy (1999), A basinwide estimate of vertical mixing in the upper pycnocline: Spreading of bomb tritium in the North Pacific Ocean, *J. Phys. Oceanogr.*, *29*, 1759–1771.

Li, X. (2003), Constraining the North Atlantic circulation with transient tracer observations, Ph.D. thesis, MIT/WHOI Joint Program, Woods Hole, Mass.

Li, X., and C. Wunsch (2003), Constraining the North Atlantic circulation between 4.5°S and 39.5°N with transient tracer observations, *J. Geophys. Res.*, *108*(C10), 3318, doi:10.1029/2002JC001765.

Marotzke, J., R. Giering, K. Zhang, D. Stammer, C. Hill, and T. Lee (1999), Construction of the adjoint MIT Ocean General Circulation Model and application to Atlantic heat transport sensitivity, *J. Geophys. Res.*, *104*, 29,529–29,547.

Mémery, L., and C. Wunsch (1990), Constraining the North Atlantic circulation with tritium data, *J. Geophys. Res.*, *95*, 5239–5256.

Messias, M.-J., C. Andrie, L. Memery, and H. Mercier (1999), Tracing the North Atlantic Deep Water through the Romanche and Chain fracture zones with chlorofluoromethanes, *Deep Sea Res., Part I*, *46*, 1247–1278.

Morse, P. M., and H. Feshbach (1953), *Methods of Theoretical Physics*, McGraw-Hill, New York.

Munk, W. (1981), Internal waves and small-scale processes, *Evolution of Physical Oceanography*, edited by B. A. Warren and C. Wunsch, pp. 264–291, MIT Press, Cambridge, Mass.

Rhein, M., O. Plaehn, R. Bayer, L. Stramma, and M. Arnold (1998), Temporal evolution of the tracer signal in the Deep Western Boundary Current, tropical Atlantic, *J. Geophys. Res.*, *103*, 15,869–15,883.

Rhein, M., J. Fischer, W. M. Smethie, D. Smythe-Wright, R. F. Weiss, C. Mertens, D.-H. Min, U. Fleischmann, and A. Putzka (2002), Labrador Sea Water: Pathways, CFC inventory, and formation rates, *J. Phys. Oceanogr.*, *32*, 648–665.

Robbins, P. E., J. F. Price, W. B. Owens, and W. J. Jenkins (2000), The importance of lateral diffusion for the ventilation of the lower thermocline in the subtropical North Atlantic, *J. Phys. Oceanogr.*, *30*, 67–89.

Roether, W., and G. Fuchs (1988), Water mass transport and ventilation in the northeast Atlantic derived from tracer data, *Philos. Trans.R. Soc. London, Ser. A*, *325*, 63–69.

Smethie, W. M., Jr., and R. A. Fine (2001), Rates of North Atlantic Deep Water formation calculated from chlorofluorocarbon inventories, *Deep Sea Res., Part I*, *48*, 189–215.

Smethie, W. M., Jr., R. A. Fine, A. Putzka, and E. P. Jones (2000), Tracing the flow of North Atlantic Deep Water using chlorofluorocarbons, *J. Geophys. Res.*, *105*, 14,297–14,324.

Stammer, D., C. Wunsch, R. Giering, C. Eckert, P. Heimbach, J. Marotzke, A. Adcroft, C. N. Hill, and J. Marshall (2002), The global ocean state during 1992–1997, estimated from ocean observations and a General Circulation Model, *J. Geophys. Res.*, *107*(C9), 3118, doi:10.1029/2001JC000888.

Stammer, D., C. Wunsch, R. Giering, C. Eckert, P. Heimbach, J. Marotzke, A. Adcroft, C. N. Hill, and J. Marshall (2003), Volume, heat, and freshwater transports of the global ocean circulation 1993–2000, estimated from a general circulation model constrained by World Ocean Circulation Experiment (WOCE) data, *J. Geophys. Res.*, *108*(C1), 3105, doi:10.1029/2001JC001218.

Vautard, R., M. Beekmann, and L. Menut (2000), Applications of adjoint modelling in atmospheric chemistry: Sensitivity and inverse modelling, *Environ. Modell. Software*, *15*, 703–709.

Veronis, G. (1972), On properties of seawater defined by temperature, salinity and pressure, *J. Mar. Res.*, *30*, 227–255.

Wanninkhof, R. (1992), Relationship between wind speed and gas exchange over the ocean, *J. Geophys. Res.*, *97*, 7373–7382.

Weiss, R. F., J. L. Bullister, R. H. Gammon, and M. J. Warner (1985), Atmospheric chlorofluoromethanes in the deep equatorial Atlantic, *Nature*, *314*, 608–610.

Wunsch, C. (1996), *The Ocean Circulation Inverse Problem*, Cambridge Univ. Press, New York.

Wunsch, C. (2002), Oceanic age and transient tracers: Analytical and numerical solutions, *J. Geophys. Res.*, *107*(C6), 3048, doi:10.1029/2001JC000797.

X. Li, Applied Ocean Physics and Engineering Department, Woods Hole Oceanographic Institution, Woods Hole, MA 02543, USA. (xli@whoi.edu)

C. Wunsch, Department of Earth, Atmospheric and Planetary Sciences, Massachusetts Institute of Technology, Cambridge, MA 02139, USA.